Formation Characteristics of microbubble in a co-flowing liquid in microfluidic chip

Hui Zhang[1], Hongwei Qin[1], Shengyuan Jiang[1*], Peng Li[1], Lixia Sun[2] and Yukun Ren[1]

[1]Harbin Institute of Technology, Harbin, Heilongjiang, 150001, China
[2]Beihua University, Jilin, Jilin, 132013, China

jiangshy@hit.edu.cn

Abstract: Microbubble formation under the surroundings of co-flowing liquid (CFL) in a specially designed microfluidic chip was investigated. A new microfluidic chip utilizing several capillary tubes was fabricated to provide the co-axial flowing conditions. An experiment platform based on high-speed microscopic camera system (HSMCS) was designed and set up. The influences of nitrogen pressure and liquid flow rate on detachment distance and volume variation of target microbubble were studied experimentally. Experimental data and analysis results indicated that the detachment distance of target microbubble decreases substantially as the rate of CFL increases while it is almost independent of nitrogen pressure. Additionally, the volume growth rate of target microbubble almost keeps constant under fixed nitrogen pressure. The present study provides empirical references for studies in microbubble formation in microfluidic chips which contributes to realize the accurate controllability in diameter and size distribution of microbubble.

1. Introduction

Microbubble dispersions have widespread applications in various technological processes including chemical engineering, environment, biological science and drug delivery [1]. For the high complexity of bubble formation, lots of attempts have been made to isolate some parameters systematically and to investigate them both theoretically and experimentally.

In the past, lots of techniques including agitation emulsification [2-4], aeration diffusers [5,6], ultrasonic cavitation [7,8] have been applied in the production of microbubble dispersions. Distinctively, conventional agitation emulsification method which adopts various special designed structures and cavities introduces gas from the ambient surroundings into the liquid solution to produce stable microbubbles.

However, microbubbles generated by above-mentioned techniques have large diameters and non-uniform size distribution. Meanwhile, such devices are generally uncompetitive in energy consumption and size controllability of microbubbles. On the contrary, the demand of quantitatively generated microbubbles which have uniform size distribution increases sharply in chemical engineering, biology science and medical researches [9,10].

Since 1970s, lots of experimental and theoretical investigations on the formation of bubbles in millimeter scale have been conducted. Both spherical and non-spherical theoretical models have been proposed to describe the formation process of single bubble, including one-stage models [11-13], two stage models [14,15], multi-stage models [16] and non-spherical models [17-19]. Meanwhile, series of experiments were performed by Liu [20], Takahashi [21], Yu [22], Koichi Terasaka [23], Najafi [24] and Bhunia [25] to investigate the phenomena of bubble formation in quiescent and flowing liquid.

Despite of above-mentioned numerous theoretical and experimental investigations of bubble formation, the mechanism of bubble growth and detachment at submerged orifices remains far from fully understood [26], especially for bubble formation under special boundary conditions.

Mostly, in current theoretical studies in bubble formation, in order to predict the final bubble volume at detachment, the detachment conditions of target bubble are usually empirically assumed that the distance between nozzle tip and geometrical center of bubble reaches a certain value [27], such as R_b+R_i where R_b and R_i represents the radius of the bubble at detachment and the inner wall of nozzle respectively, R_b+R_E where R_b and R_E represents the radius of the bubble at detachment and at the end of first stage ends respectively and so on.

The aforementioned studies on bubble formation have mostly focused on millimeter-scale bubbles that grow from a millimeter-scale nozzle or orifice. Evidences are urgently needed to indicate if there exist differences in the formation process for bubbles in millimeter and micrometer scales. Therefore, detailed studies on microbubble formation are urgently needed.

Microfluidic chips are used to produce microdroplets or microbubbles in a wide range of applications, particularly when the expected size and size distribution of droplets or bubbles are strictly prescribed on the microscale. Numerous studies on microfluidic chips or lab-on-a-chip mostly focus on microdroplets, which are widely used in biotechnology, medical applications and materials science [28-30]. However, the mechanism of microbubble formation from a microscale orifice surrounded by co-flowing liquid (CFL) in microfluidic chip is still unknown. The co-flowing liquid is hereafter referred to as CFL in the present study.

Mohammad and his co-workers [31] introduced a cost-effective microchannel fabrication method that is capable of generating microbubbles. Yan [32] reviewed the methods for microdroplets or microbubbles generation; she analyzed the typical flow regime, the forces and impact factors during droplet or bubbles formation in a T-junction microchannel. Avishay Bransky [33] proposed a microfluidic system based on a piezoelectric actuator to generate droplets, their system was able to independently control the droplet size, rate of formation and distance between droplets whose uniformity was especially high with deviation from the value by less than 0.3%.

The objective of the present study is to analyze the effect of nitrogen pressure and the rate of co-flowing liquid hereafter called CFL on the formation of target microbubble. A new microfluidic chip based on several microscale capillary tubes was designed and fabricated. Detailed experimental works were conducted with HSMCS to investigate detachment distance (DD) and volume variation of target microbubble. Useful conclusions about DD and volume variation were proposed innovatively on the basis of experimental data and analysis results.

2. Experimental work

2.1 Microfluidic chip

A new microfluidic chip which consists of three capillary tubes was designed and fabricated to provide a co-flowing liquid condition and generate microbubbles in stable size and fixed frequency. All experiments were conducted by bubbling compressed nitrogen into the microfluidic chip through a silicon capillary tube with a circular cross section.

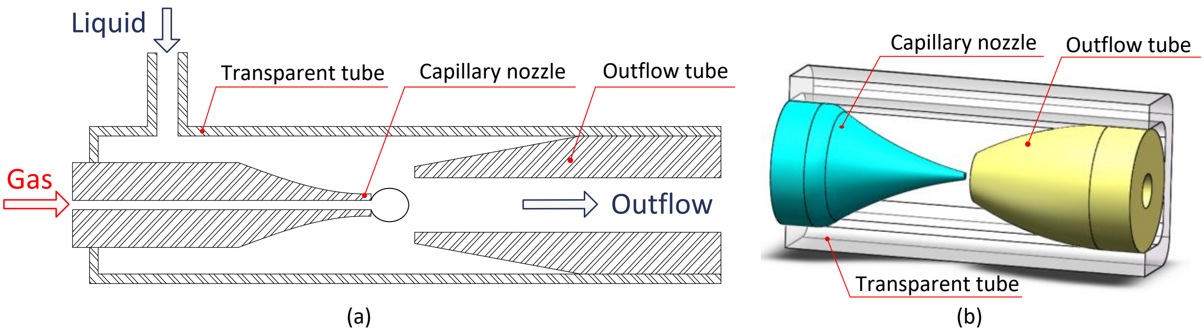

Figure 1. Schematic of the special-designed microfluidic chip.

Figure 1 shows the schematic of the special-designed microfluidic chip. Both capillary nozzle and outflow tube with a tapper tip were drawn from a commercially available capillary matrass using a Pipette Puller (Sutter P97, SUTTER INSTRUMENT) with different pulling parameters to obtain different inner diameter (ID). The inner diameters of capillary nozzle and outflow tube were 3 μm and 200 μm respectively. The inner dimension of the transparent tube was 1 mm×1mm. The maximum outer diameter of capillary nozzle was 1 mm, that is, the outline of its cross section is the inscribed circle of the inner square cross section of transparent tube. All of tubes were connected rigidly together with silicone rubber glue to ensure proper sealing of the whole microfluidic chip.

2.2 Experiment setup

As shown in figure 2, the experimental system based on HSMCS was mainly composed by a syringe pump (704500, Harvard Apparatus), a new-designed microfluidic chip as above described, a high-speed camera (Phantom V12, 100w fps), a microscope (CKX41, Olympus), a nitrogen cylinder, a regulator and a preprocessing computer. During all of experiments, syringe pump was used to pump 2 wt% polyvinyl alcohol (PVA) solution as the flowing liquid in the two-phase system of microbubble formation.

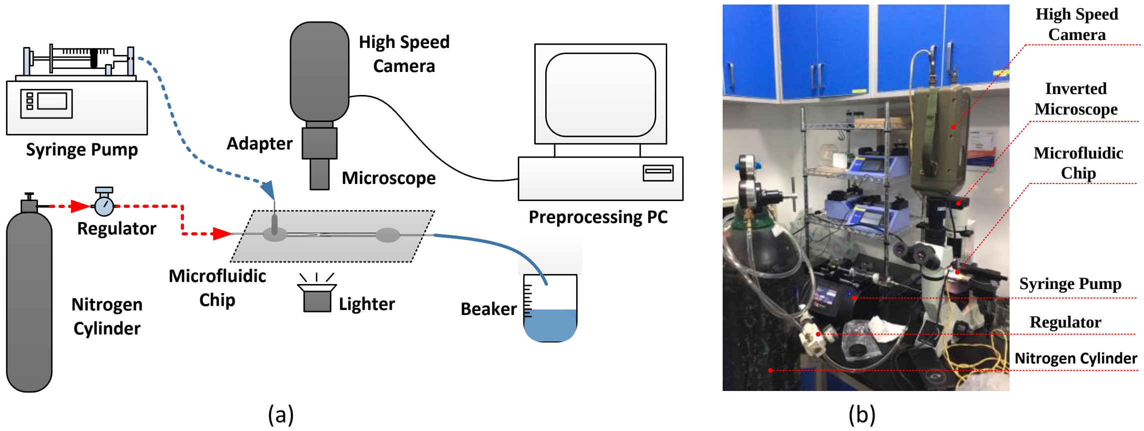

Figure 2. The constitutions of the experimental system, including: (1) high-speed camera: Phantom v12.0; (2) inverted microscope: CKX41, Olympus; (3) nitrogen cylinder; (4) specially designed microfluidic chip; (5) regulator; (6) preprocessing computer; (7) syringe pump: 704500, Harvard Apparatus.

As the inner gas, nitrogen was supplied by a compressed cylinder through the regulator to ensure that nitrogen flowed into the microfluidic chip with constant pressure. The formation and detachment of target microbubble were recorded by a high-speed camera at 10,000 frames per second.

2.3 Experimental process

Using above-described experimental system, a series of experiments were performed to study the effect of the rate of CFL and nitrogen pressure on microbubble formation. Nitrogen pressure was set as 0.1 MPa, 0.2 MPa, 0.3 MPa, 0.4 MPa, and 0.5 Mpa respectively while the rate of CFL was set as 25 mL h^{-1}, 35 mL h^{-1}, 45 mL h^{-1}, 55 mL h^{-1}, and 65 mL h^{-1} respectively. Parameters used in all experiments and their values are shown in table 1.

Table 1. Experiment parameters and their values

Parameter	Value	Parameter	Value
ID of capillary tube: d_i	3 μm	Surface tension coefficient: γ	0.0138 N m^{-1}
Liquid density: ρ_L	900 kg m^{-3}	Gas pressure: P_g	0.1-0.5 MPa
Gas density: ρ_g	1.1452 kg m^{-3}	Liquid flow rate: Q_L	25-65 mL h^{-1}
Liquid dynamic viscosity: μ_L	0.734×10^{-3} Pa·s	Liquid kinematic viscosity: ν	0.816 × 10-6 m^2 s^{-1}

3. Experimental results and discussion

3.1 Detachment distance (DD)

The detachment distance (DD) was defined as the distance between the microbubble center and nozzle tip at the moment of detaching which was measured with the software of Image Pro Plus (IPP) and hereafter referred to as DD or DDs. The 2D and 3D schematic of DD is shown in figure 3.

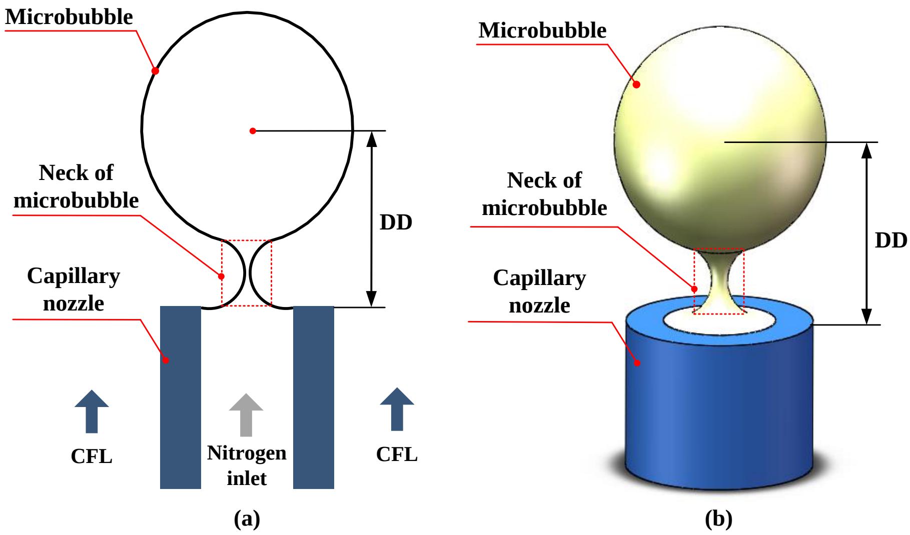

Figure 3. Detachment distance of target microbubble

In the present experimental studies, DDs of microbubbles under different generation conditions including nitrogen pressure and liquid flow rate were measured carefully. Measured results are listed in table 2 and analysis curves are shown in figure 4.

Table 2. Detachment distance (DD) of microbubble under different conditions

DD/μm	0.1 MPa	0.2 MPa	0.3 MPa	0.4 MPa	0.5 MPa
25 mL h^{-1}	39.42	41.34	41.73	42.50	40.57
35 mL h^{-1}	35.55	36.71	35.55	35.16	34.01
45 mL h^{-1}	31.68	32.07	32.84	31.30	32.07
55 mL h^{-1}	27.43	28.59	30.14	30.52	30.91
65 mL h^{-1}	25.89	26.27	24.73	27.43	28.59

On the basis of data and curves of DDs, it is obvious that the effect of nitrogen pressure on DD is much weaker than the effect of CFL. DD of microbubble decreases sharply as the rate of CFL increases while the nitrogen pressure almost has no influence on DD of microbubble and this remaining weak effect is ambiguous.

As mentioned in the current studies, surface tension, pressure force, nitrogen momentum and drag force that liquid viscidity and CFL introduce mainly affect the formation of microbubble. Therefore, this difference in impact capacity between liquid flow rate and nitrogen pressure may result from the main role which CFL plays during the formation process of microbubble.

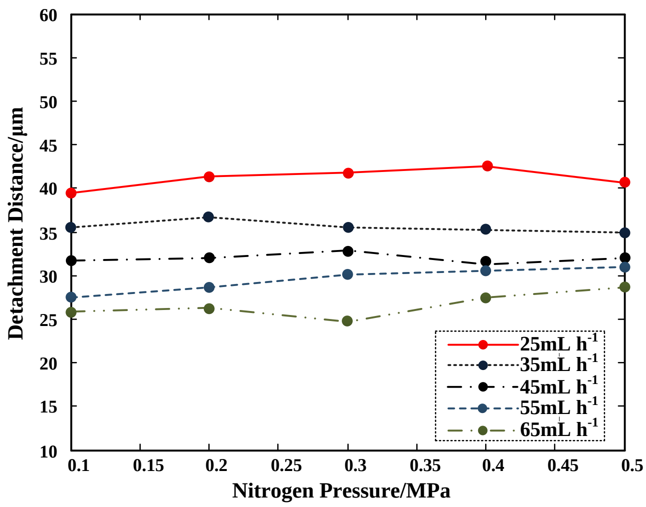

Figure 4. Variation of DD as nitrogen pressure under different rate of CFL.

On the basis of aforementioned analysis, for each rate of CFL, the average value of DD under different nitrogen pressures could be applied in any theoretical model proposed by researches of microbubble formation under the action of CFL. Most importantly, the accurate time node of microbubble detachment could be obtained by utilizing above conclusions. Meanwhile, it provides references for studies on microbubble formation affected by other flowing liquid such as countercurrent and crosscurrent flowing liquids which are widely used in microfluidic chips.

3.2 Microbubble volume

The volume of microbubble during its formation was measured and calculated with the image processing toolbox of MATLAB and the thought of calculus was adopted.

The image process program in MATLAB is as follows: original image of target microbubble was read into MATLAB; original image was transformed into gray-scale map; im2bw function in MATLAB was adopted to make threshold segmentation; the hole inside microbubble was eliminated by changing gray value of these pixels from 1 into 0.

The volume calculation program of target microbubble is introduced as follows: along the axis direction of target bubble, numbers of micro cylinders were obtained by dividing the whole body of microbubble into N pieces, then the whole volume of bubble body could be got as these micro volumes were added up.

$$V_i = \pi d^2 H / (4N)$$

where, V_i is the total volume of target microbubble; H is the height of target microbubble along the axis of capillary tube; d is the diameter of each piece of micro volume; N is the number of pieces that the whole length of H was divided. The volume calculation method of target microbubble is shown in figure 5.

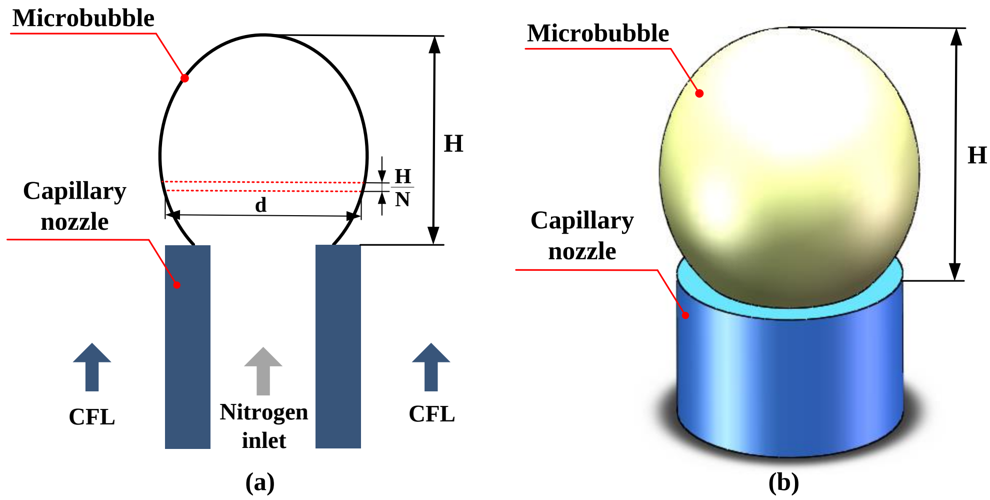

Figure 5. Volume calculation method of target microbubble

Figure 6 shows the volume of target microbubble varies as time under different nitrogen pressure with the rate of CFL: 35mL h^{-1}. It could be observed that the volume of target microbubble almost increases linearly as time under each nitrogen pressure. Meanwhile, the volume growth rate of target microbubble which was represented by the slope of the each line increases substantially as nitrogen pressure was raised and the whole time of microbubble formation reduces sharply as the figure shows. Furthermore, it's noteworthy that the effect of nitrogen pressure on the final volume of target microbubble was not clearly enough because of the fluctuation in vertical coordinate among end points of these curves.

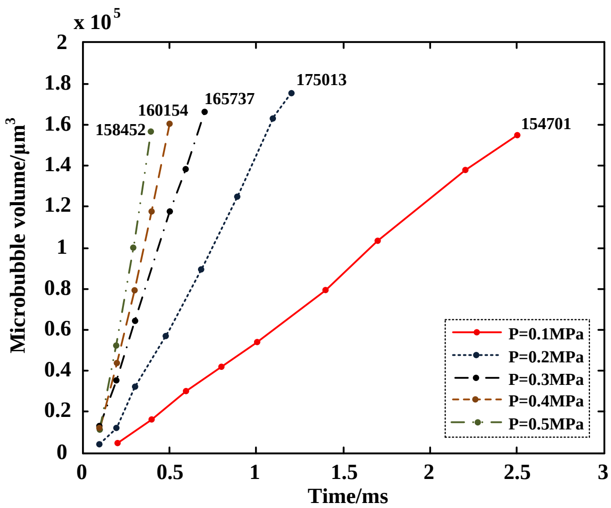

Figure 6. Measured volumes of target microbubble variation curves as time under different nitrogen pressure with the rate of CFL: 35mL h^{-1}.

The above-mentioned phenomena may result from the nearly constant flow rate of nitrogen under each pressure which may be caused by the almost non-existent chamber volume of nitrogen before it pours into liquid surroundings. Additionally, as the system pressure increases, more nitrogen enters the body of target microbubble in unit time which gives rise to the higher volume growth rate of target microbubble.

Figure 7 shows the volume of target microbubble varies as time under different rate of CFL with nitrogen pressure: 0.2 MPa. It shows from another point of view that the volume of target microbubble increases almost linearly as time under different rate of CFL. Most importantly, it is easy to figure out that the growth rates of target microbubble volume are nearly independent of the rate of CFL because of the almost same slope among these lines. What the rate of CFL affects most is that the final value of the target microbubble volume for the different end points of these lines which indicates CFL can reduce both the final volume of target microbubble and the whole time of microbubble formation.

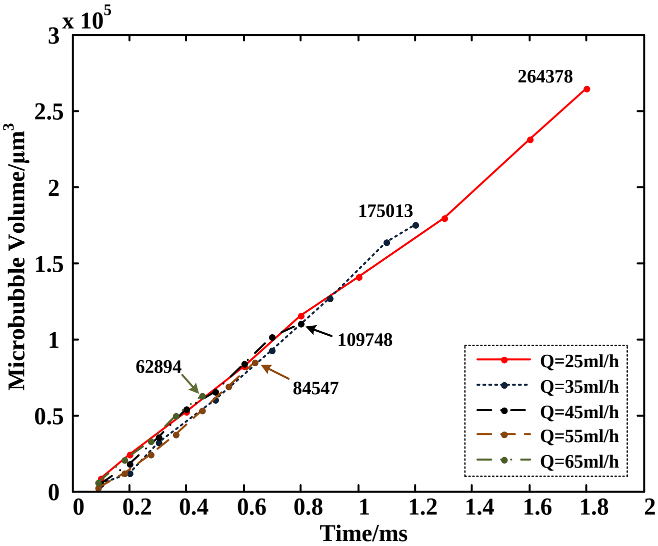

Figure 7. Measured volumes of target microbubble variation curves as time under different rate of CFL with nitrogen pressure: 0.2 MPa.

4. Conclusion

In the present study, formation of microbubble surrounded by CFL in a specially designed microfluidic chip was investigated experimentally. Two significant parameters: detachment distance (DD) and volume of target microbubble have been focused on and studied in details.

Through experimental data and analysis results, conclusions can be obtained:

(1) DD of microbubble decreases sharply as the rate of CFL increases while the nitrogen pressure almost has no influence on it which may result from the main role of liquid viscidity and CFL during microbubble formation. Accurate time node of microbubble detachment could be obtained by utilizing above conclusions and it could be applied in current theoretical models which now adopt various assumed detachment conditions.

(2) Volume of target microbubble almost increases linearly as time under each nitrogen pressure when the CFL is fixed and under different rate of CFL when nitrogen pressure is fixed. Its growth rate increases substantially as nitrogen pressure was raised while the CFL almost has no influence on it. Furthermore, formation time of target microbubble is controlled by nitrogen pressure and meanwhile the final volume is mostly affected by CFL.

Results of the present study vastly enhance our understanding of the formation mechanism of a single microbubble surrounded by CFL. Analysis programs and conclusions of this study provide references for both theoretical and experimental studies in microbubble formation under different flowing liquid. Furthermore, possibilities of controlling microbubble formation in high degree are introduced and further works on this goal will be conducted in the future.

References

[1] D. Gerlach, G. Biaswas, *Int. J. Heat Mass Transfer.* 2005, **48**(2), 425-438.
[2] Pan.Li, H.Tsuge. *J. Chem. Eng. Jpn.*, 2006, **39**(8), 896–903.
[3] M.Sadatomi, A. Kawahara, F. Matsuyama, T. Kimura. *Multiphase Sci. Technol.*, 2007, **19** (4), 323–342.

[4] Michio Sadatomi, Akimaro Kawahara. Exp. *Therm. Fluid Sci.*, 2012, **41**(4), 23–30.
[5] S. Fujikawa, R. Zhang, et.al. *Int. J. Multiphase Flow*, 2003, **29**(8), 1221–1236.
[6] Masato Kukizakia,Masahiro Gotob. *J. Membr. Sci.*, 2006, **281**(1-2), 386–396.
[7] Toshinori Makuta, Ryodai Suzuki. *Ultrasonics*, 2013, **53**(1): 196–202.
[8] Toshinori Makuta, Fumio Takemura. *J. Fluid Mech.*, 2006, **541**(1), 113.
[9] George M. Whitesides. *Nature*, 2006, **442**(7101), 368-373.
[10] Kanaka Hettiarachchi. *Lab Chip*, 2007, **7**(4), 463.
[11] Chuang, S. C. and V. W. Goldschmidt, Trans. *ASME, J. Basic Eng*., 1970, **92**(4), 705-711.
[12] R. S. Hassani, S. Chikh, *Int. J. Mech, Aero, Ind, Mech and Manu Eng.*, 2014, **8**(5), 866-868.
[13] C. Liu, B. Liang, S. Tang, H. Zhang, Chin. *J. Chem. Eng.*, 2010, **18**(5), 770-776.
[14] Avijit Bhhunia, Salvatore C. Pais, *AIChE Journal.*, 1998, **44**(7), 1499-1509.
[15] M. Martin, F. J. Montes, *Chem. Eng. Sci*, 2006, **61**(16), 5196-5203.
[16] Xianxian Yu, Yiwei Wang, *CAV2015, Journal of Physics: Conference Series*, 2015, **656**(4).
[17] KOICHI TERASAKA, HIDEKI TSUGE, *THE CANADIAN JOURNAL OF CHEMICAL ENGINEERING*., 1999, **77**(3), 458-464.
[18] Aref Seyyed Najafi, Zhenghe Xu, *Chem. Eng. Sci.*, 2008, **63**(7). 1779-1787.
[19] MARIUSZ R. RZASA, Arch. *Thermodyn.*, 2014, **35**(2), 21-36.
[20] C. Liu, B. Liang, S. Tang, H. Zhang, *Chin. J. Chem. Eng.*, 2010, **18**(5), 770-776.
[21] Takahashi, T., T. Miyahara, S. Senzai and H. Terakado, *Kagaku kogaku Ronbunshu.*, 1980, **6**(6), 563-569.
[22] Xianxian Yu, Yiwei Wang, *CAV2015, Journal of Physics: Conference Series*, 2015, **656**(4).
[23] KOICHI TERASAKA, HIDEKI TSUGE, *THE CANADIAN JOURNAL OF CHEMICAL ENGINEERING*., 1999, **77**(3), 458-464.
[24] Aref Seyyed Najafi, Zhenghe Xu, *Chem. Eng. Sci.*, 2008, **63**(7). 1779-1787.
[25] Avijit Bhhunia, Salvatore C. Pais, *AIChE Journal.*, 1998, **44**(7), 1499-1509.
[26] R. S. Hassani, S. Chikh, *Int. J. Mech, Aero, Ind, Mech and Manu Eng*., 2014, **8**(5), 866-868.
[27] Francesca Scargiali. *Chem. Eng. Technol*, 2014, **37**(9), 1507-1514.
[28] P.GARSTECKI, A.M. GANAN-CALVO, *Bull. Pol. Acad. Sci.: Tech. Sci.*, 2005, **53**(4), 163-181.
[29] Pingan Zhu, Xin Tang, *Microfluid. Nanofluid.*, 2016, **20**(3), 46-54.
[30] W. B. CHEN, REGINALD, *J. Chem. Eng. Jpn.*, 2002, **35**(10), 952-962.
[31] Mohammad Beshad Shafii, Shapour Shirani, *J. Fluids Eng*., 2013, 034501, **135**(3).
[32] Qu Yan, *Energy Conservation Technology*., 2014, **32**(5). 447-451.
[33] Avishay Bransky. *Lab Chip*, 2009, **9**(4), 516-520.